

# Ionic Interactions and Transport Properties in Methyl Terminated Poly(propylene glycol)(4000) Complexed with $\text{LiCF}_3\text{SO}_3$

Anders Ferry

Department of Physics, Umeå University, 901 87 Umeå, Sweden

Received: September 9, 1996; In Final Form: October 29, 1996<sup>®</sup>

Alternating current (ac) impedance, restricted diffusion, and vibrational spectroscopic (Raman and IR) measurements have been conducted on complexes of methyl capped poly(propylene glycol) of molecular weight 4000 and  $\text{LiCF}_3\text{SO}_3$  salt. The relative concentrations of anions in different chemical environments have been calculated from an analysis of the symmetric anion  $\text{SO}_3$  stretch (Raman) over a wide concentration range. Comparisons are made to previous studies on hydroxyl capped PPG systems, and we find that polar polymer end groups play an important role in the solvation of the salt. The relative fraction of anions interacting directly with lithium cations is considerably higher over the entire concentration range in the present study, and we infer the existence of negatively charged ionic aggregates in the solutions. We also note that the fraction of spectroscopically “free” anions increases with increasing salt concentration in the ether oxygen to alkali metal cation ratio (O:M) range 502:1 to 12:1, contrary to a decrease reported for the analogue hydroxyl terminated electrolytes. The ionic conductivity has a more pronounced concentration dependency in the methyl capped system; notably, the molar conductivity ( $\Lambda$ ) increases dramatically with increasing salt concentration passing through a relatively sharp maximum at O:M = 20:1 at room temperature. Restricted diffusion data are also reported which show that the salt diffusion coefficient increases by approximately 60% between O:M 40:1 and 20:1. The results are discussed in terms of ionic interactions and ion transport in nonideal polymer ion conductors. We comment on the characteristic concentration dependency of  $\Lambda$  and observations of low and even negative cationic transference numbers in similar complexes.

## Introduction

Ion conducting polymers, i.e., polymer electrolytes, can be obtained by dissolving salts in suitable polar polymers.<sup>1–3</sup> Because of the great potential of solid polymer ion conductors for applications in various electrochemical devices,<sup>4</sup> these materials have been intensively investigated during the past decade. A basic understanding has evolved regarding the salt and host structures that give high ionic conductivity along with the requirements to obtain chemical and mechanical stability;<sup>5</sup> however, in order to optimize the transport properties of these materials, it is desirable to elucidate the microscopic processes involved in the ionic conduction mechanism and, in particular, the mechanisms governing the long-range transport of cations.

Ionic migration in a polymer matrix is fundamentally different from that in organic liquid or aqueous electrolytes where unconstrained solvent sheaths typically surround solvated ions, thus creating distinct kinetic entities.<sup>6</sup> In a polymer electrolyte cations coordinate to polar sites in the host polymer matrix, forming more or less labile bonds, while the anions normally are not solvated by the aprotic host but occupy voids in the system.<sup>7</sup> Due to the relatively low dielectric constant of most polymer solvents, typically  $\epsilon_r \sim 5$ , long-range Coulomb forces give rise to extensive ion–ion interactions and in general several different types of ionic species can be present in the polymer–salt complexes, e.g., “free” anions, solvated cations, solvent separated ion pairs, contact ion pairs, triple ions, and higher order aggregates. Since the host matrix is relatively immobile, long-range cationic transport must involve dissociative steps where solvated cations are transferred between neighboring coordination sites<sup>8</sup> in combination with migration and diffusion of ionic aggregates weakly coordinated to the polymer solvent.

It has been shown that ionic conduction mainly occurs in amorphous regions of the polymer–salt complexes and that local polymer segmental motion plays an important role in the transport mechanism.<sup>8–11</sup> The strong coupling to the local dynamics of the solvent contributes to the complexity of the ionic transport mechanism and, along with extensive ionic interactions present in the solutions, distinguishes polymeric ion conductors from ordinary liquid electrolytes.

The concentration dependency of the molar conductivity,  $\Lambda$  (ionic conductivity normalized by the total salt concentration), in liquid electrolytes based on low-permittivity solvents has been thoroughly studied by several authors,<sup>12–14</sup> and an observed increase from a minimum at low salt concentrations with increasing concentration has been explained in terms of changes in the relative number of charge carriers. Also in most polymer electrolytes a minimum is observed in  $\Lambda$  in the low-salt concentration region at  $\sim 0.01 \text{ mol dm}^{-3}$  (O:M  $\approx 2000:1$ )<sup>15–18</sup> followed by a maximum at higher concentrations. In these studies poly(propylene glycol) of molecular weight 4000, PPG-(4000), has frequently been used as a model system for high molecular weight solid polymer electrolytes.<sup>16–18</sup> The ratio  $\Lambda_{\text{max}}/\Lambda_{\text{min}}$  varies considerably, depending on the complexing salt and the nature of the polymer containing the polyether segments; ratios up to 30 at room temperature have been reported for  $\text{NH}_4\text{CF}_3\text{SO}_3$ –PPG(4000) complexes.<sup>18</sup> The variation in  $\Lambda$  from a minimum through a maximum has been interpreted in terms of a relative increase in the number of current carrying species, in analogy with the liquid electrolytes. Such changes in the ionic speciation with increasing salt concentration have been attributed to two different effects: either through redissociation of ion pairs<sup>19</sup> or through the formation of charged triplets from ion pair–“free” ion interactions<sup>20</sup> or a combination of both. The decrease observed above the maximum is generally attributed to a reduced polymer segmental

<sup>®</sup> Abstract published in *Advance ACS Abstracts*, December 15, 1996.

mobility with increasing salt concentration, which reduces the ionic mobility, and in part to an increased ion aggregation.

Conductivity data provide no specific information on the nature of the charge carriers involved in the conduction process. Therefore, it is essential to also consider the cationic transference number,  $t^0_+$ . (By definition, a transference number is the net number of moles of an ion constituent that crosses a reference plane fixed with respect to the solvent when 1 F of current is passed perpendicular through the reference plane.) Determinations of  $t^0_+$  in polymer electrolytes are generally experimentally cumbersome or rely on assumptions about the ideality of the solution. In direct investigations, using the Hittorf method or derivatives thereof, values of  $t^0_+$  considerably less than unity, even negative in some cases, have been reported for low-molecular weight liquid polymer electrolytes<sup>21,22</sup> as well as for high-molecular weight PEO based complexes.<sup>23–25</sup> Notably, in a recent study on a PPG(4000)–LiN(CF<sub>3</sub>SO<sub>2</sub>)<sub>2</sub> system, the characteristic maximum in the molar conductivity was observed at a concentration corresponding to a negative  $t^0_+$ .<sup>22</sup> Low values of  $t^0_+$  imply that the ionic conductivity is largely anionic in nature and that migration of solvated “free” cations makes a small contribution to the overall charge transport or is balanced by a flux of negatively charged aggregates. We note in passing that there is ample precedent for negative cationic transference numbers in aqueous electrolytes.<sup>26</sup> Ingram and co-workers have previously interpreted low cationic transference numbers in terms of a relative immobilization of solvated cations through intramolecular solvation by the host matrix.<sup>21</sup>

Microscopic details of the ion–ion and ion–polymer interactions can be monitored using vibrational spectroscopic techniques (i.e., Raman and IR).<sup>27–47</sup> In particular, observed shifts and splittings of characteristic vibrational modes of the triflate anion have been related to various associations of ions.<sup>27,28,32,33,36,37,41,42,46</sup> Ion–polymer interactions are manifested as changes in spectral regions associated with polar sites of the host polymer, i.e., ether oxygens and hydroxyl terminal groups in the case of PPG.<sup>34,35</sup> Changes in the Raman active disordered longitudinal acoustic mode (D-LAM) of the polymer backbone upon solvation of salts have been interpreted in terms of a reduced segmental mobility at higher salt concentrations.<sup>31,32</sup> Spectroscopic evidence of redissociation<sup>33,47</sup> as well as increasing ion aggregation<sup>31,37</sup> with increasing salt concentration has previously been reported. Still, in a study of PPG(4000)–LiCF<sub>3</sub>SO<sub>3</sub> the relative amounts of different ionic species in the solution were found to remain approximately constant in the concentration region corresponding to an observed increase in  $\Lambda$  by a factor  $\sim 14$ .<sup>16,32</sup> Similar findings can be inferred from the data reported by Schantz.<sup>37</sup> However, for the electrolytes based on PPG(4000) in the earlier studies<sup>16–18,27–32,37</sup> the ratio of OH end groups to ether oxygens is  $\sim 1:35$ , and thus cations, as well as anions, may also coordinate to these polar end groups. In fact, it has been reported that cations coordinated to OH terminal groups are more stable than cations coordinated to ether oxygens in the polymer chains.<sup>38–40</sup> Thus, in order to use a low-molecular weight polymer, such as PPG(4000), as a model for high-molecular weight systems, it is essential to reduce the influence of such specific end group effects.

Returning to the molar conductivity, the rapid increase with increasing salt concentration has also been interpreted in terms of an enhancement of the mobility of ions coordinated to the host matrix, rather than in terms of speciation effects.<sup>30,32</sup> According to this interpretation, an increasing extent of ion–ion interactions with increasing salt concentration, assisted by the continuous reorientation of the polymer segments, promotes the migration of charge carriers. Differences in the lifetimes of associated ionic species have also been suggested to affect

the concentration dependency of  $\Lambda$  in the series MCF<sub>3</sub>SO<sub>3</sub>–PPG(4000) (M = Li, Na, NH<sub>4</sub>, ND<sub>4</sub>).<sup>30</sup>

In an attempt to elucidate the influence of ion–ion interactions on transport properties and in the interest of understanding observations of low and even negative cationic transference numbers in various polymer electrolyte systems, we have conducted ac impedance, restricted diffusion, and vibrational spectroscopic (Raman and IR) measurements on complexes of methyl capped poly(propylene glycol) of molecular weight 4000 and LiCF<sub>3</sub>SO<sub>3</sub> salt.

We will report spectroscopic data which show that the methyl capped PPG–LiCF<sub>3</sub>SO<sub>3</sub> system is highly nonideal with extensive ion–ion interactions present over the concentration range corresponding to a rapid increase in  $\Lambda$ . Restricted diffusion measurements show that the salt diffusion coefficient,  $D_s$ , increases by 60% when the O:M ratio goes from 40:1 to 20:1, which approximately matches the observed increase in  $\Lambda$ . A slight redissociation effect is observed with increasing salt concentration in the Raman data, contrary to studies on analogue hydroxyl capped systems.<sup>32,37</sup> Yet, we conclude that the observed dramatic increase in  $\Lambda$  with increasing salt concentration above  $\Lambda_{\min}$  is not a result of changes in the relative number of charge carriers as determined using vibrational spectroscopic techniques.

From a detailed analysis of the Raman active  $\nu_s(\text{SO}_3)$  and  $\delta_s(\text{CF}_3)$  modes we infer the existence of negatively charged associations of ions in the present system. Considering the low  $t^0_+$  values reported for various polymer electrolytes,<sup>21–25</sup> we propose that long-range cationic transport in some systems predominantly involves correlated motions of anions and cations, possibly in the form of weakly solvated negatively charged aggregates. Our proposal is supplementary to general evidence that ion–ion interactions strongly influence the charge transport in typical ion conducting polymer–salt complexes.

## Experimental Section

**Sample Preparation.** Methyl capped PPG(4000) was obtained by treating PPG (Aldrich Chemical Co. Inc.; MW = 4000) with dimethyl sulfate (Aldrich) at 0 °C in an ethylene glycol dimethyl ether (glyme) solution.<sup>48</sup> Before use the polymer was carefully freeze dried using repeated pump–thaw cycles, as described previously.<sup>18</sup> Lithium triflate (Aldrich) was dried under vacuum at 80 °C for 24 h and at 120 °C for another 24 h.

Comparisons of infrared spectra of the methyl capped PPG and the original hydroxyl capped polymer indicated an efficiency of the end capping process better than 90%, as determined from the relative intensity of the characteristic hydroxyl infrared band envelope at  $\sim 3500\text{ cm}^{-1}$ . Ac impedance measurements on the pure methyl capped polymer showed that the ionic conductivity at 80 °C was approximately  $\sim 10^{-9}\text{ S}\cdot\text{cm}^{-1}$ , e.g., somewhat lower than values previously reported for pure PPG(4000).<sup>16</sup>

Polymer–salt complexes were prepared in a dry helium atmosphere, the oxygen level being less than 10 ppm, by complexing methyl capped PPG(4000) with LiCF<sub>3</sub>SO<sub>3</sub> for concentrations in the range O:M = 502:1 to 12:1. Samples with O:M ratios in the range 100:1 to 502:1 were prepared by successive dilution of a batch with composition O:M = 40:1; more concentrated solutions were prepared by direct weighing where the salt was first dissolved in acetonitrile whereafter the polymer was added. Acetonitrile was removed by drying the final electrolytes under vacuum at 100 °C for 100 h. From a plot of the integrated Raman scattered intensity of the SO<sub>3</sub> symmetric stretch region at  $\sim 1025\text{--}1055\text{ cm}^{-1}$  (normalized to the intensity of the CH<sub>2</sub> region  $\sim 2900\text{--}3200\text{ cm}^{-1}$ ), the accuracy of the concentrations below O:M = 40:1 was estimated

to be within 5% of the stated values, as determined from the weighing and dilution processes.

**Vibrational Spectroscopy.** FT-Raman and FT-IR spectra were recorded at room temperature (295 K) using a Bruker IFS 66 with a Raman module FRA 106 and a near-infrared YAG laser with wavelength 1064 nm. Quartz cuvettes were loaded and sealed off in a dry box and were placed in an evacuated temperature control unit during measurements. In order to optimize the measurement time with respect to peak separation and signal to noise ratio, Raman spectra were recorded at a resolution of  $3.0\text{ cm}^{-1}$  using the Happ–Genzel apodization function. All spectra are averages of several recordings with a total number of scans varying from 4000 to approximately 100 000 (total recording time ranging from 7 to 150 h). Infrared spectra with a resolution of  $2\text{ cm}^{-1}$  were recorded at room temperature using CaF windows.

To analyze the band envelope of the  $\nu_s(\text{SO}_3)$  mode of the triflate anion (Raman), the spectrum of the pure polymer was subtracted from the spectra of the polymer–salt complexes. The  $\nu_s(\text{SO}_3)$  region was analyzed using a three component model (Gaussian shapes for the bands at  $\sim 1042$  and  $\sim 1052\text{ cm}^{-1}$  and a Voigt function for the band at  $\sim 1032\text{ cm}^{-1}$ ), including a linear background term. The error in the determined relative area of the various peaks was estimated for each set of experimental data by varying the fitting parameters. The band shape analysis was performed using Peakfit software.<sup>49</sup> A similar three component analysis was also applied to the  $\delta_s(\text{CF}_3)$  deformation mode at  $\sim 750\text{--}765\text{ cm}^{-1}$  (Raman).

**Ac Impedance Measurements.** Cells with blocking platinum electrodes were loaded and thoroughly sealed in a dry helium atmosphere. Ionic conductivities were measured for temperatures ranging from 25 to  $85^\circ\text{C}$  using a Solartron Schlumberger SI 1286 electrochemical interface and 1254 four-channel frequency response analyzer. A potential difference of 10 mV was applied to the sample at frequencies ranging from 65 000 Hz to 1 Hz. The ionic conductivity was obtained from ac impedance data, plotted in the form of a complex–plane plot (Nyquist). The ohmic resistance of the cell was taken to be the estimated high-frequency intercept of the real axis. Strict temperature control was maintained in a convection oven.

**Restricted Diffusion.** Restricted diffusion measurements were carried out entirely in a dry helium atmosphere at  $25^\circ\text{C}$  using a symmetric  $\text{Li/P(PO)}_n\text{--LiCF}_3\text{SO}_3\text{+Celgard/Li}$  cell. The polymer electrolyte was placed between lithium foils, separated by a porous disk of Celgard of  $130\text{ }\mu\text{m}$  thickness which was meticulously wetted with the electrolyte. The symmetric cells were polarized in galvanostatic mode using a computer controlled system (Mac Pile).<sup>50</sup> Current densities of  $0.03\text{--}0.05\text{ mA/cm}^2$  were used with typical polarization times in the range 15–30 min. The salt diffusion coefficient was determined for each sample from the exponential decay of the potential across the cell at long times after the current was turned off. As determined from conductivity data supplied by the manufacturer, potential tortuosity effects imposed on the diffusivity by the porous Celgard disk were disregarded.

## Results

**Ionic Conductivity.** A logarithmic plot of the ionic conductivity vs reciprocal temperature is shown in Figure 1. The temperature dependency of conductivity data for polymer electrolytes is usually analyzed using the Vogel–Tammann–Fulcher (VTF) phenomenological relationship:

$$\sigma(T) = A_\sigma T^{-1/2} \exp[-E_a/k_B(T - T_0)] \quad (1)$$

In eq 1  $A_\sigma$  is a constant related to the number of charge carriers,  $E_a$  is the pseudo-activation energy related to polymer segmental

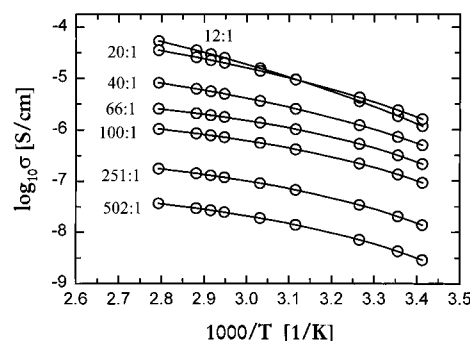


**Figure 1.** Logarithmic plot of ionic conductivity vs reciprocal temperature. Solid lines represent a fit to the VTF equation. Fitting parameters are summarized in Table 1 as a convenience for the reader.

**TABLE 1: VTF Fitting Parameters**

O:M	$c$ (mol/kg)	$A_\sigma$ ( $\mu\text{S K}^{1/2}/\text{cm}$ )	$T_0$ (K)	$E_\sigma/k_B$ (K)
502	0.034	7.3	235	290
251	0.068	35.0	235	290
100	0.167	186	235	275
66	0.252	406	239	254
40	0.402	5640	212	525
20	0.758	45 140	207	637
12	1.165	787 000	182	1166

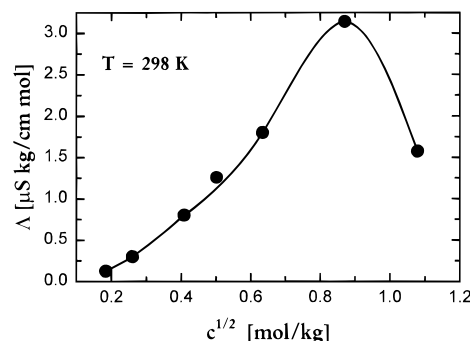


**Figure 2.** Molar conductivity at 298 K. The line is drawn as a guide to the eye.

motion, and  $T_0$  is a reference temperature usually associated with the ideal glass transition temperature at which free volume disappears. Generally speaking, the VTF relation holds at higher temperatures and is a signature of the coupling between ionic transport and polymer segmental motion. The fitted VTF parameters are summarized in Table 1. For the two most dilute samples,  $T_0$  was set equal to the value obtained for the O:M = 100:1 composition (235 K). Notably, the  $T_0$  values are anomalous and do not mirror the expected increase in the glass transition temperature with increasing concentration. Similar discrepancies have been reported for the analogue hydroxyl capped systems by Albinsson et al.<sup>16</sup> and were attributed to a strong temperature dependency of the number of charge carriers in the system. However, because of the limited temperature range, and ambiguities concerning the interpretation of these parameters,<sup>16</sup> we refrain from drawing any conclusions on the observed trends. We note that the fitted parameter  $A_\sigma$  is consistently lower in this study as compared to the results reported by Albinsson et al.<sup>16</sup> In Figure 2 the molar conductivity at  $25^\circ\text{C}$  is shown. There is a strong concentration dependency where  $\Lambda$  increases with increasing salt concentration, passing through a maximum at O:M = 20:1. The magnitude of the maximum molar conductivity is very similar to that reported for the analogue hydroxyl capped system, though the observed maximum in the present study is sharper and shifted to higher concentrations. The highest room temperature conductivity ( $\sim 2.4 \times 10^{-6}\text{ S}\cdot\text{cm}^{-1}$ ), observed at O:M = 20:1, closely

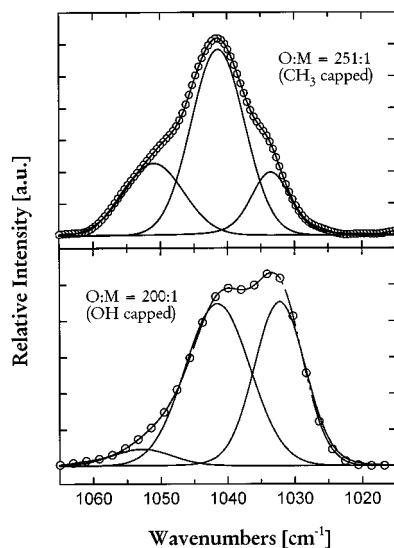


**Figure 3.** Top part: Raman spectrum of the symmetric  $\text{SO}_3$  stretch region for the O:M = 250:1 complex. Solid lines represent a three component curve fit. The spectrum has been corrected for a linear background term. Bottom part: The same spectral region for the analogue hydroxyl capped system of composition O:M = 200:1 recorded at a slightly lower resolution ( $3.5 \text{ cm}^{-1}$ ).

matches the highest corresponding value reported for the hydroxyl capped electrolyte.<sup>16</sup>

The concentration range investigated does not extend to the very low concentrations ( $\sim \text{O:M} = 2000:1$ ), where a minimum in molar conductivity generally is observed. However, from O:M = 502:1 to 20:1,  $\Lambda$  increases by a factor of  $\sim 25$  whereafter it falls off; see Figure 2. This shows that  $\Lambda_{\text{max}}/\Lambda_{\text{min}}$  is greater for the methyl capped system than for the hydroxyl capped system, where  $\Lambda_{\text{max}}/\Lambda_{\text{min}} \sim 14$ .<sup>16</sup> The relative difference between the maximum value and the value for the lowest concentration increases with increasing temperature. We note in passing that the observed increase in  $\Lambda$  with increasing salt concentration would be even more accentuated in a plot of  $\Lambda(c)$  at constant  $T - T_g$ , thus correcting for differences in polymer segmental mobility.<sup>10</sup>

**Vibrational Spectroscopy.** In Figure 3, the symmetric  $\text{SO}_3$  region of the Raman spectrum is shown for the composition O:M = 251:1 along with a typical curve fit. As a basis for comparison, the same region is also shown for an analogue hydroxyl capped system of a similar composition. According to the literature,<sup>36,46</sup> the component observed at  $\sim 1033 \text{ cm}^{-1}$  has been assigned to “free” anions not interacting directly with lithium cations. Components at  $\sim 1042$  and  $\sim 1052 \text{ cm}^{-1}$  have been attributed to contact ion pairs and  $\text{Li}_2\text{CF}_3\text{SO}_3$  triplets, respectively.<sup>36,46</sup> However, it is not possible to distinguish between free anions and solvent separated ion pairs since the frequency shifts for the latter are expected to be small. Frech et al.<sup>46,51</sup> have also pointed out that the vibrational frequencies of the triflate anion configuration  $\text{CF}_3\text{SO}_3\text{—Li—O—SCF}_3$  may be similar to those of the ion pair due to a comparable monodentate coordination in both structures. Stevens and Jacobsson have tentatively assigned the  $1042 \text{ cm}^{-1}$  band to a mixed contribution from contact ion pairs and negatively charged triple ions.<sup>36,52</sup>

As seen in Figure 4, the multicomponent band shape of the  $\nu_s(\text{SO}_3)$  mode reveals the presence of strong ion–ion interactions in the methyl capped PPG– $\text{LiCF}_3\text{SO}_3$  system over a wide salt concentration range. From the small frequency shifts of the components assigned to associated species as the salt concentration changes (an overall change of less than  $1 \text{ cm}^{-1}$  is noted) and the indifference of the component assigned to free anions ( $\sim 1033 \text{ cm}^{-1}$ ), we conclude that we have the same type

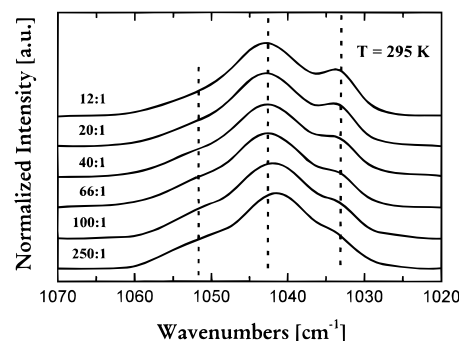


**Figure 4.** Raman spectra of the symmetric  $\text{SO}_3$  stretch region corresponding to different salt concentrations (O:M = 12:1 to 251:1). Dotted lines indicate the peak positions of the constituent bands of the most concentrated sample (O:M = 12:1).

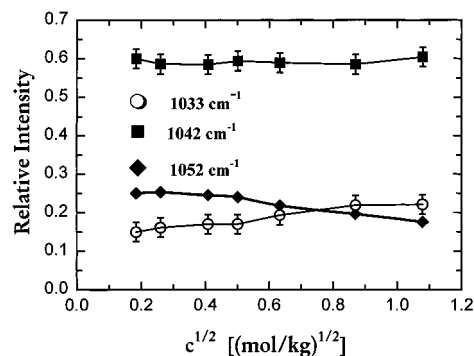


**Figure 5.** Results of a three component curve fit to the symmetric  $\text{SO}_3$  stretch region for a range of salt concentrations. Lines are drawn as a guide for the eye. Errors were estimated by varying the curve-fitting parameters.

of species present over the whole concentration range. According to Figure 4 the band at  $\sim 1033 \text{ cm}^{-1}$  increases in relative intensity with increasing salt concentration. Figure 5 shows the variation of the relative intensities of the three components with increasing concentration, as determined from a three component curve fit. We note that the relative area of the band at  $\sim 1042 \text{ cm}^{-1}$  is fairly constant at 60% and that the increase in the component at  $\sim 1033 \text{ cm}^{-1}$  corresponds to a decrease of the component at  $\sim 1052 \text{ cm}^{-1}$ . The symmetric  $\text{SO}_3$  stretch is also active in the infrared, and an analysis of the corresponding bands gives results similar to those obtained from the Raman spectra. However, the analysis of the infrared spectra is complicated by a relatively stronger concentration dependency of the polymer background.

The  $\delta_s(\text{CF}_3)$  mode of the triflate anion in the region  $\sim 750\text{—}765 \text{ cm}^{-1}$  (Raman) has also been used to estimate the relative abundance of various ionic species in other polymer–triflate salt systems.<sup>41,42,46</sup> The interpretation of observed shifts for this mode is analogous to the analysis of the symmetric  $\text{SO}_3$  stretch mode, and components at  $\sim 752$ ,  $\sim 758$ , and  $\sim 763 \text{ cm}^{-1}$  have been attributed to free anions, ion pairs, and  $\text{Li}_2\text{CF}_3\text{SO}_3$  triple ions, respectively. Figure 6 shows the Raman spectrum of this region for the composition O:M = 66:1 along with a three component curve fit. The results of an analysis along these lines agree fairly well with the results obtained for the  $\nu_s(\text{SO}_3)$  mode, though we find that the relative intensity of the band assigned to ion pairs, at  $\sim 759 \text{ cm}^{-1}$ , is somewhat greater than that of the corresponding band at  $\sim 1042 \text{ cm}^{-1}$  over the upper part of the concentration range (O:M < 40:1).

Ion–ion interactions are also manifested as shifts and splittings of the  $1272 \text{ cm}^{-1}$   $\nu_a(\text{SO}_3)$  degenerate mode in the infrared spectra. According to the literature the feature at  $\sim 1272 \text{ cm}^{-1}$  is due to free anions and is always present.<sup>40,43,44,46</sup> The bands at  $\sim 1299$  and  $\sim 1255 \text{ cm}^{-1}$  have been attributed to anions

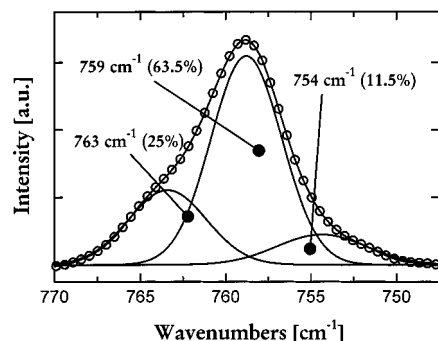


**Figure 6.** Raman spectrum of the symmetric  $\text{CF}_3$  deformation region for the O:M = 66:1 complex. Solid lines represent a three component curve fit. The spectrum has been corrected for a linear background term.

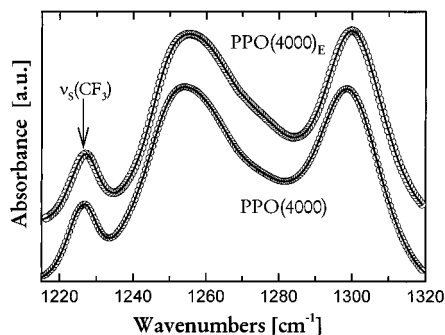


**Figure 7.** Infrared spectra of the asymmetric  $\text{SO}_3$  stretch region corresponding to methyl and hydroxyl capped PPG- $\text{LiCF}_3\text{SO}_3$  complexes, respectively. Salt concentrations: O:M = 16:1 (hydroxyl capped), O:M = 12:1 (methyl capped).

for which interactions in the solution have lifted the degeneracy of the doubly degenerate  $\text{SO}_3$  asymmetric stretch.<sup>30,40,44</sup> In Figure 7 infrared spectra of the  $\text{SO}_3$  asymmetric stretch are given for two samples corresponding to the methyl and hydroxyl capped PPG solvents, respectively. According to a four component fit, including the  $\nu_s(\text{CF}_3)$  mode at  $\sim 1225 \text{ cm}^{-1}$ , the band envelope of the  $\nu_a(\text{SO}_3)$  mode consists of components at  $\sim 1300$ ,  $\sim 1276$ , and  $\sim 1256 \text{ cm}^{-1}$  for the hydroxyl capped system. For the methyl capped electrolyte, the high- and low-frequency components are slightly shifted to higher wavenumbers ( $\sim 2 \text{ cm}^{-1}$ ), though the magnitude of the observed split is unchanged.

**Restricted Diffusion.** When a constant current is passed through the symmetric cell for a sufficient amount of time, a salt concentration gradient is established. By monitoring the potential,  $\Delta\phi$ , of the cell as the concentration profile relaxes after the current is turned off, the salt diffusion coefficient  $D_s$  can be calculated from the slope of a plot of  $\ln(\Delta\phi)$  vs time

$$\text{slope} = -\frac{\pi^2 D_s}{L^2} \quad (2)$$

where  $L$  is the thickness of the electrolyte. The theoretical analysis of the method of restricted diffusion for concentrated solutions is well-developed.<sup>53</sup> The slope must be taken after sufficient time has elapsed for linear behavior to be observed. Typical restricted diffusion data are shown in Figure 8. Due to the low conductivity of the electrolyte, only concentrations corresponding to O:M = 20:1 and 40:1 were investigated. We find that the salt diffusion coefficient for the 20:1 sample is  $\sim 2.2 \times 10^{-9} \text{ cm}^2 \text{ s}^{-1}$ , whereas for the O:M = 40 composition it is  $\sim 1.4 \times 10^{-9} \text{ cm}^2 \text{ s}^{-1}$ . Thus,  $D_s$  increases by  $\sim 60\%$  with increasing salt concentration over this concentration range. These values represent the average values for three to four experiments

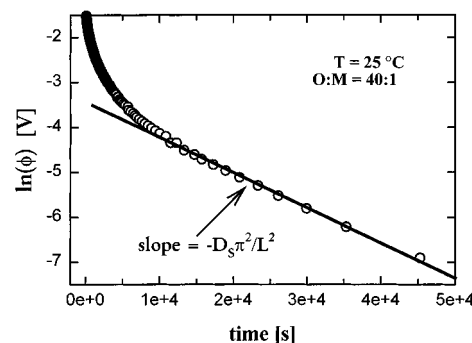


**Figure 8.** Typical restricted diffusion data (where, for example,  $1\text{e}+4$  means  $1 \times 10^4$ ). The slope is taken at long times in order for linear behavior to be observed.

for each salt concentration, and the accuracy is estimated to be better than 15%.

## Discussion

The remainder of this paper is organized as follows. First the spectroscopic data are discussed in terms of ionic interactions. Then observations regarding the influence of ionic interactions on transport properties such as ionic conductivity, transference numbers, and diffusion coefficients are reviewed. The discussion is concluded by a section where a simple model for cationic transport is outlined.

**Evidence of Ion-Ion Interactions: Influence of Polar End Groups.** As seen in Figure 5, the relative area of the band at  $\sim 1033 \text{ cm}^{-1}$  assigned to free anions is relatively small, on the order of 15–25% of the total band area over the entire concentration range investigated. This is considerably lower than what was observed in an earlier study on hydroxyl capped PPG- $\text{LiCF}_3\text{SO}_3$  complexes, where approximately 40–50% of the anions were assigned to free anions and solvent separated ion pairs over a wide concentration range.<sup>32</sup> In Figure 3 Raman spectra of the symmetric  $\text{SO}_3$  stretch region are shown for two dilute electrolytes based on the methyl capped and normal PPG-(4000), respectively. In the methyl capped system, the relative intensity of the band envelope is shifted toward the high-frequency components, assigned to ion pairs and higher aggregates,<sup>36,46</sup> as compared to the hydroxyl capped electrolyte.<sup>32</sup>

Bernson and Lindgren have previously reported changes in the characteristic infrared absorption bands corresponding to the hydroxyl end groups upon complexation with various triflate salts. Their results showed that there are specific interactions between the cations and the polar polymer end groups and also between the anions and the hydroxyl end groups.<sup>40</sup> In fact it has been reported that cations coordinated to hydroxyl end groups are more stable than cations coordinated to ether oxygens in the polymer chains.<sup>38–40</sup> Therefore it is likely that the solubility of the salt in the hydroxyl capped polymer matrix is dominated by ionic interactions with the polar end groups for low salt concentrations. This conclusion agrees with the earlier observation of a fairly constant degree of association over a wide range of concentrations in electrolytes based on hydroxyl capped PPG.<sup>32,37</sup> A relatively low fraction of free anions in the methyl capped PPG electrolytes, in comparison with systems based on methyl capped low-molecular weight PEO,<sup>47</sup> also agrees with the generally observed higher solubility of salts in PEO solvents as compared to PPG based electrolytes.<sup>54</sup>

In Figure 4 the symmetric  $\text{SO}_3$  stretch band envelope is shown normalized to unit area for a wide salt concentration range. It is seen that the relative intensity of the band at  $\sim 1033 \text{ cm}^{-1}$  increases with increasing concentration from O:M = 250:1 to 12:1. According to Figure 5, the relative intensity of the band at  $\sim 1042 \text{ cm}^{-1}$  is approximately constant over the same range

but the increase in free anions is closely matched by a decrease in the band at  $\sim 1052\text{ cm}^{-1}$ . This observation indicates that aggregated ionic species dissociate with increasing salt concentration. In fact, it has earlier been proposed that an increase in the permittivity of the electrolyte with increasing salt concentration can reduce the association constant and hence cause a redissociation of ion pairs.<sup>55</sup> In this context we note that Prud'homme and co-workers previously have suggested that PPG based electrolytes consist of complexed salt rich microdomains of a fixed composition dispersed in a salt-free polymer matrix.<sup>56</sup> Such microphase separation could explain the relatively weak concentration dependency of the degree of association of the salt previously reported for electrolytes based on PPG(4000).<sup>31,32,37</sup> However, in the present study the distribution of local anionic environments is concentration dependent, as seen in Figures 4 and 5.

Figures 3–5 show that the relative intensity of the band assigned to  $\text{Li}_2\text{CF}_3\text{SO}_3$  triplets ( $\sim 1052\text{ cm}^{-1}$ ) is larger than that of the band assigned to free anions for O:M ratios of 40:1 and lower concentrations. It has previously been suggested that the component at  $\sim 1042\text{ cm}^{-1}$  also has a contribution from negatively charged triplets.<sup>36,46,51,52</sup> On the basis of the assignments by Frech et al.<sup>46</sup> for the bands at  $\sim 1032$  and  $1052\text{ cm}^{-1}$  and the requirement of charge neutrality in the solution, we infer the existence of such negatively charged aggregates in this system at low salt concentrations. The argument is supported by the possibility of a substantial contribution from solvent separated ion pairs to the band at  $\sim 1032\text{ cm}^{-1}$ .<sup>33</sup> An alternative interpretation would be to attribute the high-frequency component ( $1052\text{ cm}^{-1}$ ) to larger aggregates. However, such complexes are expected at higher salt concentrations and have previously been assigned<sup>52</sup> to a band at  $\sim 1076\text{ cm}^{-1}$  which is not observed in this study.

Similar arguments can also be used regarding the interpretation of the  $\delta_s(\text{CF}_3)$  mode of the triflate anion in the region  $\sim 750\text{--}765\text{ cm}^{-1}$  (Raman). Figure 6 shows a large feature at  $\sim 759\text{ cm}^{-1}$ , assigned to ion pairs, along with two smaller components at  $\sim 752$  and  $\sim 763\text{ cm}^{-1}$  which have been assigned to free anions and  $\text{Li}_2\text{CF}_3\text{SO}_3$  triplets, respectively.<sup>41,42,46</sup> Largely overlapping bands due to the relatively small shifts of this mode complicate the analysis, but as seen in Figure 6 the relative intensity of the high-frequency component is greater than that assigned to free anions. Thus, the feature at  $\sim 759\text{ cm}^{-1}$  may also have a contribution from negatively charged aggregates. The finer structure of the  $\delta_s(\text{CF}_3)$  mode seen in Figure 6 is not observed in the hydroxyl capped system where only a broad band at  $\sim 759\text{ cm}^{-1}$  is present.<sup>48</sup> This observation indicates that triflate anions interact directly with the polar end groups in the hydroxyl terminated PPG–electrolytes, thus masking shifts due to ion–ion interactions.

Other evidence for extensive ionic interactions in both the methyl capped and the hydroxyl capped electrolytes can be inferred from the infrared spectra of the asymmetric  $\text{SO}_3$  stretch region at  $\sim 1240\text{--}1300\text{ cm}^{-1}$ . Figure 7 shows infrared spectra of electrolytes corresponding to the hydroxyl and methyl capped PPG hosts, respectively. There is some disagreement in the literature about the assignment of the bands observed at  $\sim 1272$ ,  $\sim 1300$ , and  $\sim 1255\text{ cm}^{-1}$ , but it is generally agreed that the components at  $\sim 1255$  and  $\sim 1300\text{ cm}^{-1}$  correspond to splits of the asymmetric  $\text{SO}_3$  stretch mode at  $\sim 1272\text{ cm}^{-1}$  caused by a lowering of the symmetry for the anion through interactions in the solution.<sup>57</sup> The bands at  $\sim 1255$  and  $\sim 1300\text{ cm}^{-1}$  have also been assigned to contact ion pairs, where the magnitude of the splitting has been related to the strength of the interaction; the larger the splitting the stronger the ionic interaction.<sup>33,44</sup> The feature at  $\sim 1272\text{ cm}^{-1}$  has been attributed to free anions, though

it may also have a contribution from solvent separated ion pairs.<sup>43</sup> However, even though specific assignments have been made for this mode,<sup>46</sup> this spectral region is not suitable for quantitative estimates of the relative amounts of various species since the absorption coefficients vary for the different components.<sup>33</sup> Returning to Figure 7, the great differences between the methyl and hydroxyl capped systems seen in the Raman spectra of the  $\nu_s(\text{SO}_3)$  and the  $\delta_s(\text{CF}_3)$  modes are not reflected in the infrared band envelope of the asymmetric  $\text{SO}_3$  stretch. This further indicates that the usefulness of this mode for quantitative purposes is limited.

**Ionic Transport and Ionic Interactions.** There is substantial evidence that ion transport in polymer electrolytes is intimately coupled to the segmental mobility of the polymer host matrix.<sup>9–11</sup> Notably, models describing the transport process in terms of noninteracting particles diffusing in a continually redistributed host matrix, such as the dynamic bond percolation model,<sup>8</sup> generally recover the characteristic VTF temperature dependency of the ionic conductivity.

However, the characteristic concentration dependency of  $\Lambda$  clearly highlights the importance of particle interactions in typical polymer electrolytes. By combining analytical results, based on the dynamic bond percolation model,<sup>8</sup> with Monte Carlo simulations, Ratner and co-workers<sup>58</sup> showed that ionic conductivity in a simple lattice model is diffusion dominated even in the presence of Coulomb interactions between ions. Still, the generally observed increase in  $\Lambda$  from a minimum at low concentrations with increasing salt concentration could not be retrieved, which suggested that solvation effects influence the concentration dependency in real systems.<sup>58</sup>

In a simple description of the ionic conductivity, neglecting the dynamic nature of the ion–ion interactions,  $\Lambda$  can be expressed as a sum over the contributions from the different charge carriers according to:

$$\Lambda = \sum_i \alpha_i \mu_i q_i \quad (3)$$

where  $\alpha_i$ ,  $\mu_i$ , and  $q_i$  refer to the relative concentration, mobility, and charge of the  $i$ th species respectively. An extended version of eq 3 has been derived by Payne et al.,<sup>59</sup> from the exact formulation of Caillol et al.<sup>60,61</sup> for dc conductivity in a nonpolarizable ionic solution, in order to account for cross-terms, i.e., ionic exchange between conducting species.

According to eq 3, a strong concentration dependency of  $\Lambda$  must be related to a corresponding dependency of the relative amounts of charge carriers in the system or to changes in the mobility of the various species with increasing salt concentration. However, the spectroscopic data in the present study, as well as that previously reported,<sup>32</sup> do not indicate any dramatic changes in the ionic speciation that can explain the large increase in  $\Lambda$  for PPG(4000)–triflate salt electrolytes. It can be reasoned that the slight redissociation effect observed for the methyl capped system accounts for part of the increase in  $\Lambda$  by an increasing relative number of charge carriers; yet,  $\Lambda$  increases by a factor  $\sim 25$  over the region where the fraction of spectroscopically free anions only increases by  $\sim 50\%$ . Still, in view of the discussion in the previous section, the possibility of a contribution from negatively charged triple ions cannot be ruled out since such species are indistinguishable from neutral ion pairs using spectroscopic methods.<sup>36,46,51</sup>

It is interesting to note that the concentration dependency of  $\Lambda$  is even more pronounced in the methyl capped system where specific interactions with polar end groups have been eliminated. This shows that the generally observed increase in  $\Lambda$  in PPG based electrolytes is not governed by any saturation of sites in the host polymer associated with the hydroxyl end groups. The

possibility of such a saturation of preferred cationic coordination sites has been suggested to partly explain the rapid increase in  $\Lambda$  in these systems.<sup>30</sup> However, even in the absence of polar end groups there may be a distribution of coordination sites with different lifetimes, including statistically generated "crown ether" formations and cations coordinated to both anions and ether oxygens. For instance, Petrucci et al. argue that the majority of ions exist as solvent separated ion pairs in dilute solutions of methyl capped PEO(400) and LiClO<sub>4</sub> and also infer the existence of solvent separated dimer aggregates.<sup>62</sup>

Other strong indications of the influence of particle interactions on ionic transport properties have been revealed in recent transference number measurements, using a galvanostatic method developed by Newman et al.<sup>24</sup> Most notably, the bulk sodium transference number is negative over a wide concentration range for electrolytes based on high-molecular weight PEO complexed with NaCF<sub>3</sub>SO<sub>3</sub> and NaN(CF<sub>3</sub>SO<sub>2</sub>)<sub>2</sub>.<sup>22,24,25</sup> Similar results have also been seen in a PPG(4000)–LiN(CF<sub>3</sub>SO<sub>2</sub>)<sub>2</sub> system, where the characteristic maximum in  $\Lambda$  occurs at a concentration corresponding to a negative value of  $t^0_+$ .<sup>22,25</sup> A negative cationic transference number implies that negatively charged aggregates are more mobile than positively charged clusters or cations coordinated to the polymer host. We note in passing that a net cationic current can be sustained even with a negative  $t^0_+$ , but then a large concentration gradient necessarily builds up across the cell. The importance of  $t^0_+$  for the successful operation of lithium polymer cells has been thoroughly investigated by Newman et al.<sup>63</sup>

In view of the discussion above it is interesting to note results by Arumugam et al.<sup>64</sup> for a high-molecular weight PMEO–LiPF<sub>6</sub> system where it was found that conductivities calculated from pfg NMR diffusion data using the Nernst–Einstein relation were considerably higher than what was experimentally determined. They concluded that the discrepancy involves relatively facile diffusion of uncharged ionic species. Similar observations have also been reported for low-molecular weight PEO–LiCF<sub>3</sub>SO<sub>3</sub> systems,<sup>47,65,66</sup> where the discrepancy was found to increase with decreasing salt concentration. Arumugam et al.<sup>64</sup> also conclude that rapid exchange must take place between any species of different mobility present in the system (on the time scale of the pfg NMR experiment).

Referring to the above observations, it is clear that ion–ion interactions have a great impact on the overall ionic transport in ion conducting polymer media.

**Cationic Transport in Nonideal Polymer Systems: A Simplistic Picture.** The notion of negatively charged aggregations of ions being involved in the conduction process in polymeric electrolytes has not previously received much attention, yet, considering the weak interaction of anions with aprotic solvents, it is tenable that such entities have a significant mobility despite their inherent bulky nature. For instance, Armand and co-workers<sup>67</sup> have reported consistently higher values of the diffusion coefficients for anionic species as compared to lithium ions even in the system PEO–LiC<sub>8</sub>F<sub>17</sub>SO<sub>3</sub> over a range of temperatures. The experimental<sup>47,64–66</sup> and simulated<sup>59,68</sup> indications of correlated motions of cations and anions in different polyether–salt complexes support this conjecture. In view of the proposed intramolecular solvation of cations,<sup>21</sup> the mobility of positively charged aggregates is likely to be greatly restricted in a macroscopically immobile host polymer.

Thus, one can picture a long-range cationic transport process which involves the diffusion/migration of weakly solvated ionic aggregates, in addition to the proposed dynamic bond percolation<sup>8</sup> by solvated cations. A somewhat similar "vehicular model" has previously been suggested by Armand et al. for

cation transport in electrolytes based on divalent salts.<sup>69</sup> From molecular dynamics simulations of low-molecular weight polymeric ethers, Payne et al. found that there is a substantial contribution to the overall ionic transport from neutral ion pairs and larger aggregates.<sup>59</sup> It can be argued that if cationic transport primarily involves motion of complexed ions, i.e., neutral and negatively charged aggregates, similar diffusion coefficients should be observed for the cations and anions, respectively. This is generally not observed in polymer electrolytes, where anionic species typically have significantly higher diffusion coefficients.<sup>64,67</sup> However, considering the dynamic nature of associations of ions, exchange of cations between mobile aggregates and polyether sites on the host matrix may well account for the observed differences along with the presence of free uncomplexed anions. Experimental indications of rapid ionic exchange have previously been reported for the Eu(CF<sub>3</sub>SO<sub>3</sub>)<sub>3</sub>–PPG(4000) system by Brodin et al.;<sup>70</sup> Catlow and co-workers conclude from molecular dynamics simulations that cation diffusion typically occurs by internal rearrangements of the ionic substructure, involving anionic species, assisted by the segmental motion of the polymer chains.<sup>68</sup>

Turning to the observed concentration dependent enhancement of  $\Lambda$ , this effect has been attributed to an increasing rate of exchange between various ionic species and polar sites on the polymer host matrix with increasing salt concentration<sup>30,32</sup> in conjunction with a possible saturation of preferred coordination sites.<sup>30</sup> If solvated ions at concentrations corresponding to  $\Lambda_{\min}$  predominantly are present in solvent-separated ion pair configurations,<sup>62</sup> an increasing extent of ion–ion interactions with increasing salt concentration may well enhance  $\Lambda$  by a relative reduction in the strength of the pair wise ionic interaction. We note that, at the low concentrations ( $\sim 0.01$  mol/dm<sup>3</sup>) typically corresponding to a minimum in the molar conductivity, the average distance between solvated ions is on the order of  $\sim 35$  Å, while, at O:M $\sim 20$ –40:1, corresponding to  $\Lambda_{\max}$  in the PPG based electrolytes, the average separation is  $\sim 10$ –12 Å. Considering the proximity of ions in the O:M range corresponding to the observed maximum in  $\Lambda$ , we agree with Ratner and co-workers<sup>59</sup> that the notion of distinct chemical species being involved in the conduction mechanism "may be an oversimplification that impedes understanding of the real mechanisms involved in transport".

The conjecture of an increased ionic mobility with increasing salt concentration agrees well with the observation in the present study of an increase in the salt diffusion coefficient when going from O:M = 40:1 to 20:1. The increase in  $D_s$  closely matches the observed increase in  $\Lambda$ . A correlation between the concentration dependencies of  $D_s$  and  $\Lambda$  has also been seen in a system of PPG–LiN(CF<sub>3</sub>SO<sub>2</sub>)<sub>2</sub> over a wider concentration range.<sup>22</sup> A slight increase in the lithium ion diffusion coefficient can also be inferred from the data of Arumugam et al.<sup>64</sup> on a PMEO–LiPF<sub>6</sub> system with increasing salt concentration after an initial drop from the most dilute sample investigated. It is to be noted that such concentration dependent enhancement of the ionic mobility cannot be coupled to changes in the viscosity,  $\eta$ , or the glass transition temperature,  $T_g$ . Both  $T_g$  and  $\eta$  generally increase with increasing salt concentration,<sup>16</sup> which would rather suggest a decreased ionic mobility according to Walden's rule.<sup>71</sup>

## Conclusions

There is a growing body of evidence that ionic interactions play an important role in the overall charge transport in polymer ion conductors. Polymer electrolyte systems are typically highly nonideal, and extensive ion–ion interactions are present even at very low salt concentrations.<sup>27,31–33</sup>

From our work it is clear that the presence of polar hydroxyl groups influences the ability of PPG(4000) to dissolve triflate salt. By substitution of hydroxyl end groups with methyl groups, the relative fraction of spectroscopically free anions, as observed in Raman spectra, decreases from ~45% to ~15–20% at lower salt concentrations.<sup>32</sup> From an analysis of the Raman active SO<sub>3</sub> symmetric stretch we infer the existence of negatively charged associations of ions in the present system. A slight redissociation effect is observed with increasing salt concentration. We find that the concentration dependency of  $\Lambda$  is more pronounced in the methyl capped system than what has previously been reported for analogue hydroxyl capped complexes.<sup>16</sup> In the upper concentration region corresponding to the increase in  $\Lambda$  we find that the salt diffusion coefficient increases with increasing salt concentration.

The results are discussed in terms of ionic interactions, and a simple picture of the ion transport mechanism is outlined which addresses observations of low and even negative cationic transference numbers in various polymer electrolyte systems.<sup>21–25</sup> We propose that long-range cationic transport in some polyether salt complexes predominantly involves correlated motions of cations and anions, possibly in the form of negatively charged aggregates.

**Acknowledgment.** Grants from stiftelsen Blancheflor-Boncompagnie are gratefully acknowledged as are grants from JC Kempes minnes stipendiefond. The author expresses his appreciation to Professor Lutgard De Jonghe and Dr. Marca Doeff at Lawrence Berkeley National Laboratory (LBNL) for their hospitality and use of excellent laboratory facilities. Invaluable assistance in the preparation of samples by Dr. Minmin Tian and Dr. John Kerr at LBNL is also greatly appreciated, as are valuable discussions with Dr. Per Jacobsson at Umeå university.

## References and Notes

- (1) Wright, P. V. *Br. Polym. J.* **1975**, *7*, 319.
- (2) Armand, M. B.; Chabagno, J. M.; Duclot, M. J. In *Fast Ion Transport in Solids*; Vashista, P., Mundy, J. N., Shenoy, G. K., Eds.; Elsevier North Holland: New York, 1979; p 131.
- (3) Bruce, P. G.; Vincent, C. A. *J. Chem. Soc., Faraday Trans.* **1993**, *89*, 3187.
- (4) Gray, F. M. *Solid Polymer Electrolytes*; VCH: New York, 1991; Chapter 1.
- (5) See, for instance: *Polymer Electrolyte Reviews-1* (a) and *Polymer Electrolyte Reviews-2* (b); MacCallum, J. R.; Vincent, C. A., Eds.; Elsevier: London, 1987, 1989.
- (6) See, for example: Bockris, D. M.; Reddy, A. K. N. *Modern Electrochemistry*; Plenum Press: New York, 1970; Vol. 1, p 77.
- (7) Gray, F. M. In Ref 4; p 50.
- (8) Ratner, M. A. In Ref 5a; p 173.
- (9) Harris, S.; Shriver, D. F.; Ratner, M. A. *Macromolecules* **1986**, *19*, 987.
- (10) Tipton, A. L.; Lonergan, M. C.; Ratner, M. A.; Shriver, D. F.; Wong, T. T. Y.; Han, K. J. *Phys. Chem.* **1994**, *98*, 4148.
- (11) Fontanella, J. J.; Wintersgill, M. C.; Smith, M. K.; Semancik, J.; Andeen, C. G. *J. Appl. Phys.* **1986**, *60*, 2665.
- (12) Smedley, S. I. *The Interpretation of Ionic Conductivity in Liquids*; Plenum: New York, 1980.
- (13) Davies, C. W. *Ion Association*; Butterworth: London, 1962; Chapter 10.
- (14) Fuoss, R. M.; Kraus, C. A. *J. Am. Chem. Soc.* **1933**, *55*, 2387.
- (15) Gray, F. M. *Solid State Ionics* **1990**, *40–41*, 637.
- (16) Albinsson, I.; Mellander, B.-E.; Stevens, J. R. *J. Chem. Phys.* **1992**, *96*, 681.
- (17) Albinsson, I.; Mellander, M.-E.; Stevens, J. R. *Solid State Ionics* **1993**, *60*, 63.
- (18) Albinsson, I.; Mellander, B.-E.; Stevens, J. R. *Solid State Ionics* **1994**, *72*, 177.
- (19) Cameron, G. G.; Ingram, M. D.; Sorrie, G. A., *J. Chem. Soc., Faraday Trans. 1* **1987**, *83*, 3345.
- (20) Gray, F. M. *J. Polym. Sci. B* **1991**, *29*, 1441.
- (21) Cameron, G. G.; Harvie, J. L.; Ingram, M. D. *Faraday Discuss. Chem. Soc.* **1989**, *88*, 5.
- (22) Ferry, A.; Doeff, M. M.; De Jonghe, L. C. *Electrochim. Acta*, submitted for publication.
- (23) Bruce, P. G.; Haregrave, M. T.; Vincent, C. A. *Solid State Ionics* **1992**, *53–56*, 1087.
- (24) Ma, Y.; Doyle, M.; Fuller, T. F.; Doeff, M. M.; De Jonghe, L. C.; Newman, J. *J. Electrochem. Soc.* **1995**, *142*, 1859.
- (25) Ferry, A.; Doeff, M. M.; De Jonghe, L. C.; Doyle, M. *J. Electrochem. Soc.*, to be published.
- (26) Robinson, R. A.; Stokes, R. H. *Electrolyte Solutions*, 2nd ed.; Butterworth: London, 1959; p 161.
- (27) Schantz, S.; Torell, L. M.; Stevens, J. R. *J. Chem. Phys.* **1991**, *94*, 6862.
- (28) Kakihana, M.; Schantz, S.; Torell, L. M., *J. Chem. Phys.* **1990**, *92*, 6271.
- (29) Schantz, S.; Sandahl, J.; Börjesson, L.; Torell, L. M. *Solid State Ionics* **1988**, *28–30*, 1047.
- (30) Ferry, A.; Jacobsson, P.; Stevens, J. R. *J. Phys. Chem.* **1996**, *100*, 12574.
- (31) Torell, L. M.; Schantz, S. In Ref 5b; p 1.
- (32) Ferry, A.; Jacobsson, P.; Torell, L. M. *Electrochim. Acta* **1995**, *40*, 2369.
- (33) Bishop, A. G.; MacFarlane, D. R.; McNaughton, D.; Forsyth, M. *J. Phys. Chem.* **1996**, *100*, 2237.
- (34) Wendsjö, Å.; Lindgren, J.; Paluszkievicz, C. *Electrochim. Acta* **1992**, *37*, 1689.
- (35) Yoon, S.; Ichikawa, K.; MacKnight, W. J.; Hsu, S. L. *Macromolecules* **1995**, *28*, 4278.
- (36) Jacobsson, P.; Albinsson, I.; Mellander, B.-E.; Stevens, J. R. *Polymer* **1992**, *33*, 2778.
- (37) Schantz, S. *J. Chem. Phys.* **1991**, *94*, 6296.
- (38) Torell, L. M.; Jacobson, P.; Petersen, G., *Polym. Adv. Technol.* **4** **1993**, 152.
- (39) Manning, J.; Frech, R.; Huang, E. *Polymer* **1990**, *31*, 2245.
- (40) Bernson, A.; Lindgren, J. *Polymer* **1994**, *35*, 4842.
- (41) Huang, W.; Frech, R. *Polymer* **1994**, *35*, 235.
- (42) Frech, R.; Huang, W. *Solid State Ionics* **1994**, *72*, 103.
- (43) MacFarlane, D. R.; Meakin, P.; Bishop, A.; MacNaughton, D.; Rosalie, J. M.; Forsyth, M. *Electrochim. Acta* **1995**, *40*, 2333.
- (44) Frech, R.; Huang, W. *J. Sol Chem.* **1994**, *23*, 469.
- (45) Ferry, A.; Jacobsson, P.; van Heumen, J. D.; Stevens, J. R. *Polymer* **1996**, *5*, 737.
- (46) Huang, W.; Frech, R.; Wheeler, R. A. *J. Phys. Chem.* **1994**, *98*, 100.
- (47) Ferry, A.; Orädd, G.; Jacobsson, P. *Electrochim. Acta.*, submitted for publication.
- (48) Ferry, A.; Tian, M. *Macromolecules*, in press.
- (49) Peakfit is a commercially available product from Jandel, Inc.
- (50) Chabre, Y. P. *J. Electrochem. Soc.* **1991**, *138*, 329.
- (51) Frech, R. Personal communication.
- (52) Stevens, J. R.; Jacobsson, P. *Can. J. Chem.* **1991**, *69*, 1980.
- (53) Newman, J.; Chapman, T. W. *AIChE J.* **1973**, *19*, 343.
- (54) Watanabe, M.; Ogata, N. In Ref 5a; p 39.
- (55) Cavell, E. A. S.; Knight, P. C. *Z. Phys. Chem.* **1968**, *57*, 3.
- (56) Vachon, C.; Vasco, M.; Perrier, M.; Prud'homme, J. *Macromolecules* **1993**, *26*, 4023.
- (57) See ref 30, and references cited therein.
- (58) Lonergan, M. C.; Shriver, D. F.; Ratner, M. A. *Electrochim. Acta* **1995**, *40*, 2041.
- (59) Payne, V. A.; Xu, J.-H.; Forsyth, M.; Ratner, M. A.; Shriver, D. F.; de Leuw, S. W. *Electrochim. Acta* **1995**, *40*, 2087.
- (60) Caillol, J. M.; Levesque, D.; Weis, J. J. *J. Chem. Phys.* **1989**, *91*, 5544.
- (61) Caillol, J. M.; Levesque, D.; Weis, J. J. *J. Chem. Phys.* **1989**, *91*, 5555.
- (62) Salomon, M.; Xu, M.; Eyring, E. M.; Petrucci, S. *J. Phys. Chem.* **1994**, *98*, 8234.
- (63) Doyle, M.; Fuller, T. F.; Newman, J. *Electrochim. Acta* **1994**, *39*, 2073.
- (64) Arumugam, S.; Shi, J.; Tunstall, D. P.; Vincent, C. A. *J. Phys. C* **1993**, *5*, 153.
- (65) Boden, N.; Leng, S. A.; Ward, I. M. *Solid State Ionics* **1991**, *45*, 261.
- (66) Ward, I. M.; Boden, N.; Cruickshank, J.; Leng, S. A. *Electrochim. Acta* **1995**, *40*, 2071.
- (67) Gorecki, W.; Donoso, P.; Berthier, C.; Mali, M.; Roos, J.; Brinkmann, D.; Armand, M. B. *Solid State Ionics* **1988**, *28–30*, 1018.
- (68) Catlow, C. R. A.; Mills, G. E. *Electrochim. Acta* **1995**, *40*, 2057.
- (69) Baril, D.; Chabre, Y.; Armand, M. B. *J. Electrochem. Soc.* **1993**, *140*, 2687.
- (70) Brodin, A.; Mattson, B.; Torell, L. M. *J. Chem. Phys.* **1994**, *101*, 4621.
- (71) Walden, P. *Z. Phys. Chem.* **1906**, *55*, 249.